Monika LIEDKE[1], Eugeniusz ŁOWIEC[1], Wojciech MATELSKI[2], Leszek WOLSKI[1], Ryszard STRZELECKI[1]

Instytut Elektrotechniki, Bałtycka Pracownia Technologii Energoelektronicznych w Gdyni (1), Politechnika Gdańska, Wydział Elektrotechniki i Automatyki (2)

doi:10.15199/48.2018.05.21

Selection of AHI + SC Hybrid Storage Based on Mathematical Models and Load Variation Characteristics

Abstract. *The article deals with the design of a hybrid storage consisting of Aqueous Hybrid Ion battery (AHI) and supercapacitor (SC) modules. The selection of components is based on the knowledge of the load profile of the storage and the AHI battery and supercapacitor models. The paper presents the method of selecting components of the storage made of AHI batteries and supercapacitor modules The article includes an example of the hybrid storage design intended for the supply of household electric appliances.*

Streszczenie. *Artykuł dotyczy metody projektowania zasobnika hybrydowego złożonego z baterii Aqueous Hybrid Ion (AHI) i modułów superkondensatorowych (SC). Dobór elementów opiera się na znajomości profilu obciążenia zasobnika oraz modeli baterii AHI i superkondensatora SC. W pracy przedstawiono sposób doboru elementów zasobnika złożonego z baterii AHI i modułów superkondensatorowych. W artykule zamieszczono przykład projektu zasobnika hybrydowego przeznaczonego do zasilania elektro-sprzętów gospodarstwa domowego.* ***(Dobór zasobnika hybrydowego na podstawie modeli matematycznych i charakterystyki zmienności obciążenia)***.

Keywords: hybrid storage, Aqueous Hybrid Ion battery, supercapacitor
Słowa kluczowe: zasobnik hybrydowy, bateria Aqueous Hybrid Ion, superkondensator

Introduction

With the increasing use of renewable energy sources, such as photovoltaic panels and wind turbines, there is growing interest in new ways of collecting and storing electricity. Typical solutions in this area are lithium-ion or lead-acid batteries. The main shortcomings of these examples are: limited durability, toxicity of appropriate electrolytes and components, potential fire hazard, disposal problems of waste batteries.

The new high quality component that has appeared on the market is a battery called Aqueous Hybrid Ion battery containing salt electrolyte - neutral to the environment. For a detailed description of AHI battery technology, see [1]. The materials used in the construction do not contain heavy metals and are fully recyclable as opposed to existing lead-acid, nickel-cadmium, nickel-metal hydride, sodium-sulfur, and lithium-ion batteries [2]. This component also does not present a fire hazard. In addition, the AHI battery ensures significant durability expressed by a large number of charging and discharging cycles. Due to the aforementioned advantages it is suitable for the construction of scalable storage, in particular for stationary applications. However, the disadvantage of this type of battery is the relatively large internal resistance, which complicates the assembly of a structure suited for large, pulsed charging and discharging currents. In such cases the solution may be to use an additional component in the form of a supercapacitor. This problem is the subject of many studies [3], [4], [5], [7], which point out the possibility of improving the dynamic parameters and extending the battery life. The following sections show how to create the AHI battery model and the supercapacitor model as components of the hybrid system. An example hybrid storage system, made up of AHI type S30-0080 batteries and LSUM 129R6C 0062F EA supercapacitor, was established and used for the validation of the elaborated model. The research has confirmed the good accuracy of the hybrid battery model. The paper proposes a method for selecting storage elements based on the knowledge of the load profile and elaborated model. The method is illustrated on the example of a storage that can be used to power a kitchen equipped with household electronics.

Hybrid storage

In many studies, for example: [5], [6], [7], the advantages of supercapacitor combined with chemical batteries are indicated. Direct, parallel connection is called passive hybrid. There are also configurations using DCDC converters, called active hybrid [8], [9]. Active hybrid configurations allow better use of the energy stored in the supercapacitor and/or protection of the chemical battery during charging or discharging. However, these are more expensive solutions and introduce additional energy losses. A special example of hybridization are ultra – batteries, comprised of a lead acid battery and a supercapacitor in a single cover pack [10]. However, such rechargeable batteries cause problems with optimum selection of the storage components.

AHI battery model

The basic parameters of the AHI battery are shown in table 1. For more detailed information, see the manufacturer's data sheet [11]. Based on own research and studies [12 - 15], the model is proposed as in figure 1. It consists of two parts: the electrical power circuit, as in figure 1(a) and the control circuit as in figure 1(b).

Table 1. AHI battery parameters

Cycle Life	3 000 cycles (to 70%retained capacity)
Operating Temperature	-5ºC to 40ºC ambient
Voltage Range	40,0 to 57,6 V
Nominal Voltage	48 V
Continuous Power	680 W
Peak Power	800 W
Continuous Current	17 A
Usable Depth of Discharge	100 %
Round Trip Efficiency	> 90 %
Height	935mm
Width	330mm
Depth	310mm
Weight	118kg

In the process of elaborating the model, the following assumptions were adopted:
- model parameters are temperature-independent,
- battery capacity does not depend on battery current (no Peukert effect),
- the internal resistance $R0 + R1$ is constant, independent of the State Of Charge (SOC) and of the battery current,
- the self-discharge effect is neglected,
- the resistance of the supply lines is omitted Rp = 0.

The acceptance of the temperature independence assumption is justified, when the battery is operating under normal temperature conditions.

(a)

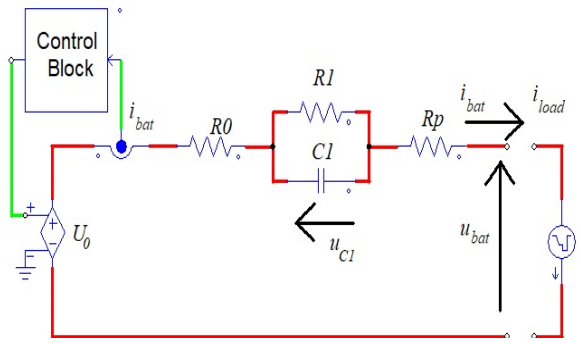

(b)

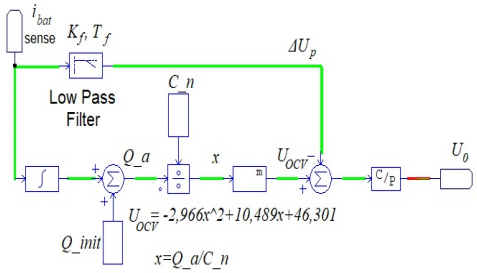

Fig.1. Mathematical model of AHI battery; a) power circuit, (b) control circuit

The signals shown in the figure 1(b) indicate: U_o- electromotive force of the source, ΔU_P - polarization voltage, Q_init - initial charge, Q_a – actual remaining charge of battery. The electrical circuit as in figure 1(a) can be represented in the form of a system of equations (1). It allows to determine the response in the form of model battery voltage u_{bat} to the change of the current i_{bat}. drawn from the battery by the load. The source voltage U_0 is assumed to be a constant.

$$\begin{aligned} \frac{du_{C1}}{dt} &= \frac{-1}{R1 \cdot C1} \cdot u_{C1} + \frac{1}{C1} \cdot i_{bat} \\ u_{bat} &= U_0 - u_{C1} - R0 \cdot i_{bat} \end{aligned} \tag{1}$$

Based on equation (1), the short-term response of the model to the change in load current i_{load} can be determined. The control circuit, as in figure 2, allows calculation of the source voltage U_0 according to formula (2):

$$\begin{aligned} & U_0 = U_{OCV}(SOC) - \Delta U_P \\ & where \\ & SOC = \frac{Q\_a}{C\_n}, \quad Q\_a = \int i_{bat} \cdot dt + Q\_init, \\ & \Delta \overline{U_P}(s) = \frac{K_f}{s \cdot T_f + 1} \cdot i_{bat}(s) \end{aligned} \tag{2}$$

where: K_f– gain of the filter, T_f– time constant, s – laplace transform variable.

The Open Circuit Voltage U_{OCV} depends on the State Of Charge (SOC) of the battery. The SOC is defined as ratio of remaining charge Q_a to the nominal charge Q_n of the battery. The U_{OCV} voltage dependency of the SOC is usually a nonlinear relation. The example of such dependency is depicted in figure 1(b). Control voltage U_0 is the sum of the U_{OCV} component, that is a function of the SOC battery charge and the ΔU_P component, depending on the average value of current $i_{bat.}$ The ΔU_P component is added, when the battery is charged, or subtracted, when it is discharged. The low-pass filter used in the model allows for polarization [12] to be taken into account. Its purpose is to rebuild the voltage on the battery terminals after the discharge current has vanished. The low pass filter reflect so called long term response of the developed model.

Calculation of model parameters

The model parameters as shown in figure 1(a) are calculated from the waveforms shown in figure 2. For this purpose, the AHI battery was discharged with 5 A DC current, which then was abruptly increased to 10 A. After 50 s the current was reduced to 5 A.

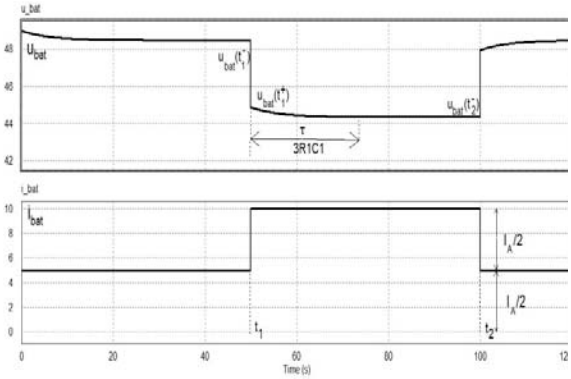

Fig.2. Battery voltage u_{bat} waveform change due to impulse current i_{bat}

Based on the registered battery response u_{bat}, according to equations (4), the parameters of the model were evaluated as in figure 1 (a).

$$\begin{aligned} R0 + R1 &= 2 \cdot \frac{u_{bat}(t_1^-) - u_{bat}(t_2^-)}{I_A} \\ R0 &= 2 \cdot \frac{u_{bat}(t_1^-) - u_{bat}(t_1^+)}{I_A} \\ C1 &= \frac{\tau}{3 \cdot R1} \qquad \tau \cong 3 \cdot R1 \cdot C1 \end{aligned} \tag{4}$$

The model parameters, as shown in figure 1(b), were determined on an experimental basis. During charging and discharging, the current and voltage of the battery were recorded. The process of charging (or discharging) was gradual. After each charging phase (discharging), there was a break (approximately) 12 h to measure the U_{OCV} voltage. Based on the recorded waveforms of the battery currents during charging or discharging, the charge Q_a, currently available in the battery, was calculated. Load Q_a was normalized to a nominal value of 48.3 Ah specified by the manufacturer. The process of loading (or discharging) was cyclical. The next steps of charging or discharging of the batteries were repeated until fully charged or discharged state was achieved. In the datasheet [16] the fully charged state of the AHI battery is considered to be at the voltage level of 57.6 V, after charging with a constant current of 2 A with the ambient temperature at 30°C. Examples of recorded battery discharge voltage and current waveforms are presented in figure 3 and figure 4. For the dependence of the U_{OCV} voltage, on the battery state of charge, see figure 5.

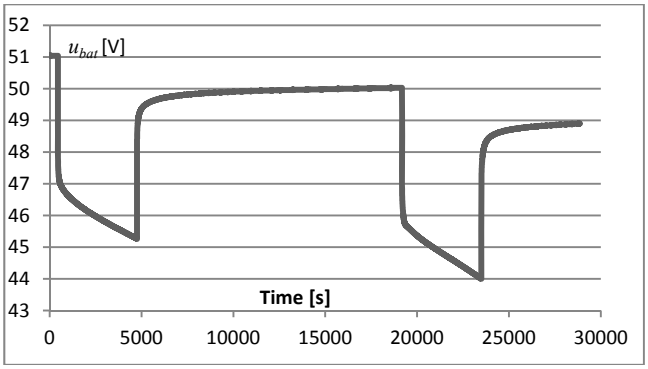

Fig.3. Voltage waveform during discharge. Two successive discharge steps

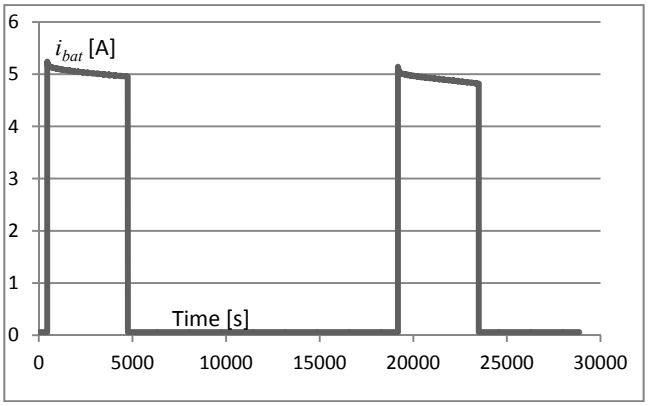

Fig.4. The current of the battery during discharge. Two successive discharge steps

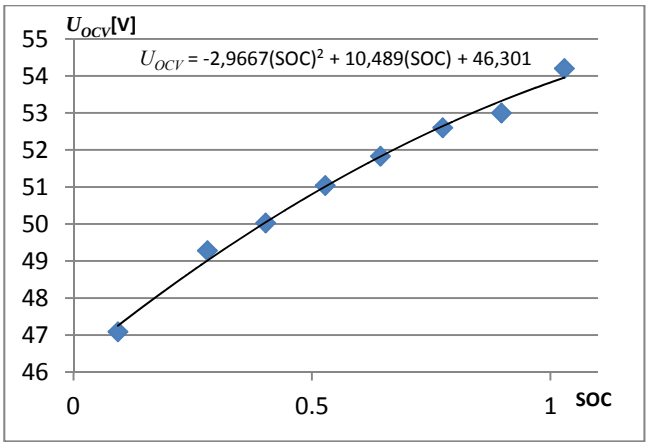

Fig.5. Voltage U_{OCV} dependency of AHI battery from State Of Charge

Based on the analysis of the battery voltage and the discharge current after successive charging phases, the time constant of the filter T_f = 10800s and the gain K_f = 0.288 were estimated. The compilation of parameters of the AHI battery model is shown in table 2.

Table 2. Parameters of model AHI battery (discharge)

Internal resistance *R0*	0.645 Ω
Polarization resistance *R1*	0.104 Ω
Polarization capacitance *C1*	56.8 F
Gain of low pass filter K_f	0.288
Time constant of low pass filter T_f	10800 s
Open Circuit Voltage U_{OCV}	-2,9667(SOC)^2 + 10,489(SOC) + 46,301 [V]

Supercapacitor model

For the construction of a hybrid storage, supercapacitor LSUM 129R6C 0062F EA was used with parameters as given in table 3.

Table 3. Supercapacitor LSUM 129R6C 0062F EA parameters

Capacitance	62.5 F	
Voltage Range	136.8 V	
Nominal Voltage	129.6 V	
Resistance	13.2 mΩ	
Stored energy	Initial	145.8 Wh
	End of life	116.6 Wh
Max. Continuous Current	ΔT=15°C	190 A
	ΔT=40°C	260A
Current	Leakage	<27 mA
Temperature	Operating	-40 ~ +65 °C
	Storage	-40 ~ +70 °C
Cycle Life (25°C)	After 1,000,000 cycles between rated voltage to half rated voltage at +25 °C	
	Capacitance change	<20% decrease
	Internal resistance change	<100% increase
Height	226 ± 1 mm	
Width	405 ± 2 mm	
Length	720 ± 4 mm	
Weight	53 ± 1 kg	

The supercapacitor model was created using the "Ultracapacitor Model Tool" [17] available in the PSIM version 10 simulation software. The circuit model of the super capacitor used by the software is shown in figure 6.

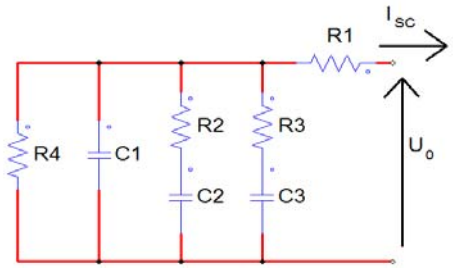

Fig.6. Electrical circuit based supercapacitor model

The elements *R1* and *C1* of the electrical circuit are responsible for the short-term (seconds) response of the model to changes in charging or discharge currents. Values of *R2*, *C2* and *R3*, *C3* elements affect respectively the average-term (minutes) and long-term (hundreds of minutes) response of the model. The resistor *R4* includes the self-discharge effect of the supercapacitor.

Determining model parameters

In order to determine the model parameters of the selected supercapacitor, the voltage variations during the processes of charging it with a constant current of I_{SC}= 50 A and selfdischarge, were recorded. The obtained data, in form of a text file, was entered into the Ultracapacitor Model Tool together with the values of the charging current I_{sc}, the maximum voltage V_{rated}, and the leakage current $I_{leakage}$. The window for communication with the simulation program is shown in figure 7.

The calculated equivalent model parameters and approximation error are displayed in the lower right part of the window. The Circuit parameters, as shown in figure 6, were: $R1$=0.052 Ω, $C1$=52.36 F, $R2$=106 Ω, $C2$=7.9 F,

R3=96.8 Ω, C3=3.24 F, R4=1129 Ω. The error of the supercapacitor model, 0.55%.

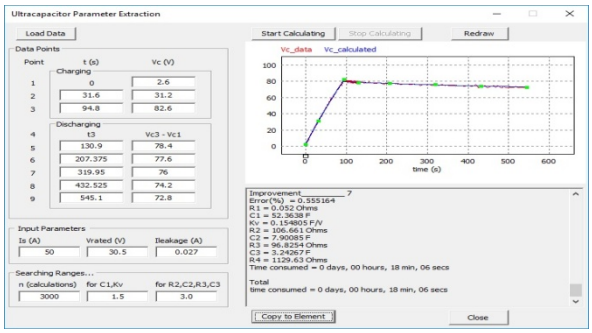

Fig 7. The "Ultracapacitor Model Tool" window in PSIM v.10.

Validation of the hybrid battery model

The scheme of the laboratory system for hybrid battery testing is shown in figure 8. The values of currents i_{bat}, i_{SC} and battery voltage u_{bat} were recorded in 1 second steps using a data logger. Impulse discharge of the battery was made by the use of the current source prepared for the experiment.

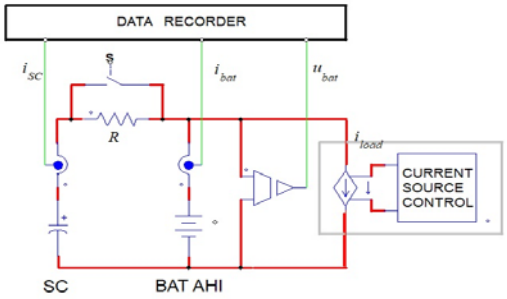

Fig. 8. Scheme for testing hybrid storage

Example waveforms of hybrid storage system voltage as a response to load current pulses drawn from the battery are presented respectively in figures 9 and 10.

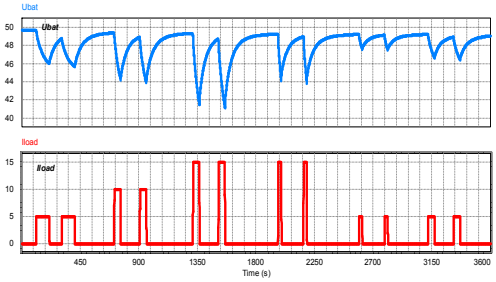

Fig.9. Voltage u_{bat} variation of the hybrid storage forced by pulse current profile i_{load} (Pulse Width 2 x 100 s, 2 x 50 s, 2 x 50 s, 2 x 25 s, 2 x 25 s, 2 x 50 s)

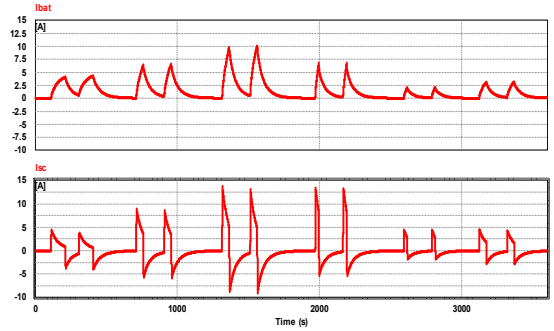

Fig.10. Current i_{bat} and i_{sc} of the hybrid storage

The resistor R allowed the limitation of the compensation currents occurring during the first connection of the supercapacitor to the battery.

In order to assess the quality of the models described, they were subject to simulation (based on the software PSIM v. 10.) - the model of the AHI battery and the supercapacitor LSUM 129R6C 0062 were connected in parallel. For the identical I_{load} in form of series I_{load} pulses, i_{bat_s}, i_{sc_s}, u_{bat_s} responses were obtained. The simulation errors in percentage were calculated by the formula (5).

$$error\_i_{bat} = \frac{i_{bat} - i_{bat\_s}}{i_N} \cdot 100\,\%$$

$$error\_u_{bat} = \frac{u_{bat} - u_{bat\_s}}{u_N} \cdot 100\,\% \quad (5)$$

$$where: i_N = 17\,A, \quad u_N = 48V$$

The results of comparing laboratory recorded waveforms with results obtained by simulation studies are shown in figure 11.

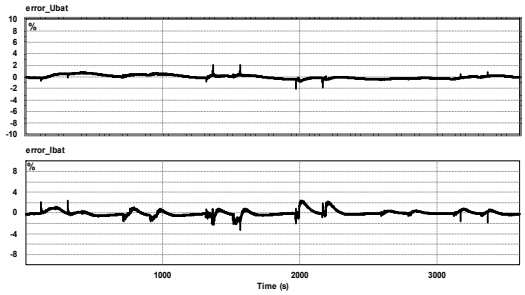

Fig. 11. Voltage and current response errors on the pulsed i_{load} current load

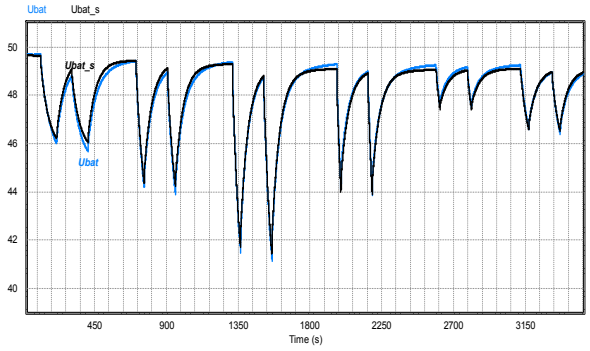

Fig. 12. Comparison of voltage response u_{bat_s} of the hybrid storage model and real response u_{bat} to the identical load profiles i_{load} *as* shown in Fig. 9

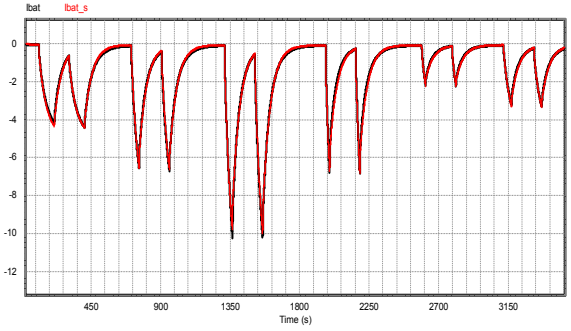

Fig. 13. Comparison of current response i_{bat_s} of the hybrid storage model and real response i_{bat} to the identical load profiles i_{load} *as* shown in Fig. 9

The impulse errors, shown in figure 11, result from the difference in the value of the registration and simulation steps. Registration of actual value u_{bat} and i_{bat} took place in 1 second steps, while signals u_{bat_s} and i_{bat_s} simulation 0.1 second steps.

The mean value of the absolute error for the period of 3600 seconds was 0.27% for the voltage u_{bat} and 0.35% for the current i_{bat}. Maximum values were 2% and 3.2% respectively. Figures 12 and 13 show the recorded waveforms and corresponding simulation results.

Method of selecting components of the hybrid storage

The hybrid storage consisted of parallel-coupled l AHI batteries and k supercapacitor modules as shown in figure 14. It was assumed, that when the hybrid storage device begins to power the load, AHI batteries and supercapacitors are fully charged and a statistically representative load profile $p_{profile}$(t) is known.

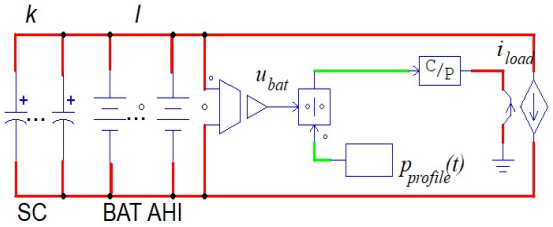

Fig.14. Hybrid storage with simulated load i_{load} based on power profile $p_{profile}$(t) *for* $t \in \langle 0, T \rangle$. T is the time, at which the hybrid storage is loaded

A statistically representative profile is chosen from the number N of all registered profiles, or which the maximum power and energy (delivered to receivers) are closest in terms of the distance d to the average power and the average energy (6).

$$\overline{P_{p\_\max}} = \frac{1}{N} \cdot \sum_{j=1}^{N} P_{p\_\max}(j)$$

$$\overline{E_p} = \frac{1}{N} \cdot \sum_{j=1}^{N} E_p(j) \tag{6}$$

$$d = MIN \sqrt{(\overline{P_{p\_\max}} - P_{p\_\max}(j))^2 + (\overline{E_p} - E_p(j))^2}$$

where:
j - number of registered profile $j \in \langle 0, N \rangle$
$E_p(j)$-energy of the j-th profile,
$P_{p\_max}(j)$-peak power of the j-th profile.

The problem of selecting components of the hybrid storage is to find such a pair of positive integers (l, k) for which the objective function in the formula (7):

$$F_C(k,l) = C_{bat} \cdot l + C_{sc} \cdot k$$

(7) *or*

$$F_M(k,l) = M_{bat} \cdot l + M_{sc} \cdot k$$

where:
C_{bat} , C_{sc} the cost of a single battery and the cost of a supercapacitor module,
M_{bat} , M_{sc} the mass of a single battery and the mass of the supercapacitor module,

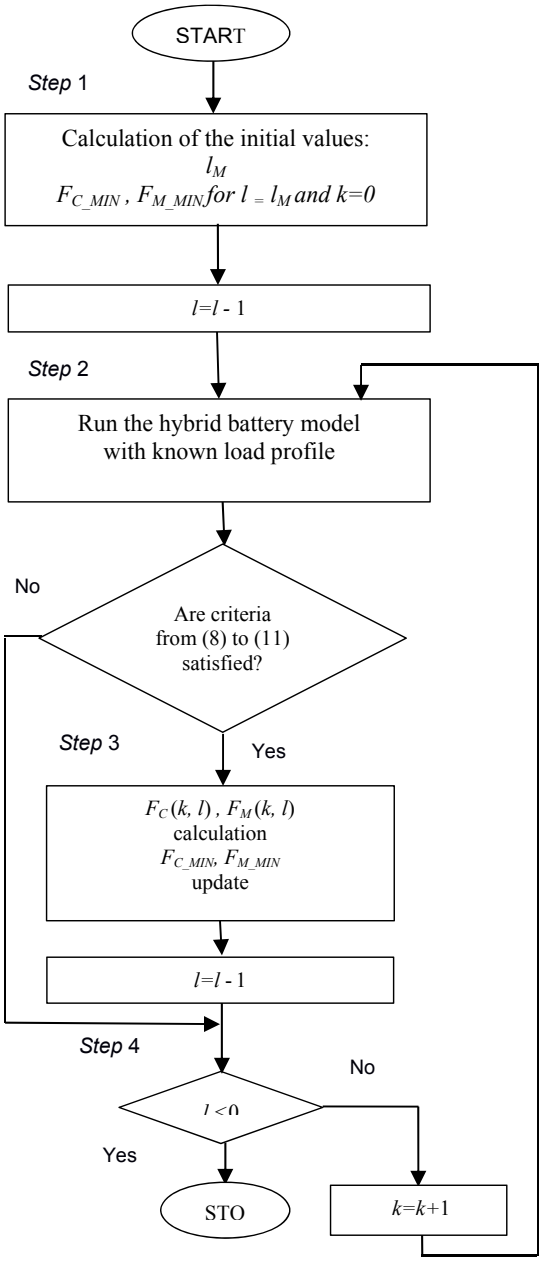

Fig.15. General block diagram of the storage element selection algorithm.

Achieves its minimum with the following restrictions:

$$l \cdot P_{bat\_\max} > \frac{1}{\eta} \cdot P_{p\_MAX}$$

(8) *or*

$$k \cdot P_{sc\_\max} > \frac{1}{\eta} \cdot P_{p\_MAX}$$

$$l \cdot E_{bat} + k \cdot E_{sc} > \frac{1}{\eta} \cdot \int_0^T p_{profile}(t)\, dt \tag{9}$$

$$i_{bat}(t) < I_{bat\_\max} \tag{10}$$

$$u_{bat}(t) > U_{bat\_min} \tag{11}$$

$$t \in \langle 0, T \rangle$$

where: P_{bat_max}, P_{sc_max} the maximum continuous power of a single battery and the maximum power of the supercapacitor, E_{bat}, E_{sc} the energy stored in a single battery and the energy stored in the supercapacitor module, $p_{profile}(t)$ the profile load, P_{p_MAX} maximum load power, T power consumption time, η efficiency of the converter between the hybrid storage and the energy receivers, I_{bat_max} the maximum current of a single AHI battery, U_{bat_min} the minimum output voltage of the hybrid battery

Condition (8), (9), (10), (11) verification is based on a model constructed as a parallel connection of l AHI battery modules and k supercapacitor modules.

The method of selecting a storage configuration for a representative power profile is presented in the form of an algorithm block diagram in figure 15.

The description of the algorithm can be presented in the following steps:

Step 1
The start value l_M is determined according to formula (12). The initial values of the objective function are calculated according to formulas (7) for $k = 0$ *and* $l = l_M$

$$F_{C\_MIN} = F_C(0, l_M)$$
$$F_{M\_MIN} = F_M(0, l_M)$$

$$l_M = MAX(a,b) + 1 \quad where:$$
$$a = Ent\left(\frac{\frac{1}{\eta}\cdot P_{p\_MAX}}{P_{bat\_max}}\right),$$
(12)
$$b = Ent\left(\frac{\frac{1}{\eta}\cdot \int_0^T p_{profile}(t)dt}{E_{bat}}\right)$$
$$Ent(.) \quad entier$$

Step 2
For new value *l*
the hybrid storage model is started and the constraints from (8) to (11) are checked. If they are satisfactory then the calculations are done in *Step 3*

Step 3
The new target function (7) values are calculated. If the newly calculated function values are less than the old values then:

if $F_{C\_MIN\_OLD} > F_C(k,l)$ then $F_{C\_MIN} = F_C(k,l)$
if $F_{M\_MIN\_OLD} > F_M(k,l)$ then $F_{M\_MIN} = F_M(k,l)$

New value of $l = l - 1$ is updated

Step 4
The termination requirement of the loop is checked. If it is satisfied, then the calculations are stopped. The F_{C_MIN}, F_{M_MIN} variables represent the minimum values of the goal functions. The values represented by the pair (l_C, k_C) or (l_M, k_M) show a configuration of the hybrid storage.

The way in which the components of the hybrid storage are selected, is based on the knowledge of the models and stochastic load profile. The use of stochastic data may, for example, lead to temporary overloading of the storage and improper operation of the powered devices. In most cases, the probability of occurrence of such an event is small and acceptable to the user.

The literature on hybrid storage design [18-20], [9] deals among others on economic aspects. Complex systems containing the presence of renewables are also considered. The effects of the use of supercapacitors mainly have impact on the prolonged life of chemical batteries and the improved dynamic properties of the hybrid storage. The active hybrid topology is preferred where supercapacitor and battery each has his own converter. The common feature of the described methods is that statistically representative load profiles, as well as renewable power source profiles, are used.

Selection of the storage elements example

The example shows how to design a storage suited to power the electrical appliances of the kitchen equipped with: microwave, coffee machine, fridge, lighting, electric kettle. It is assumed that the hybrid storage power will be maintained for 8 hours. The electrical appliances are powered from the hybrid storage by the means of a DCAC converter (48VDC / 230VAC). Scheme of the circuit is shown in figure 16.

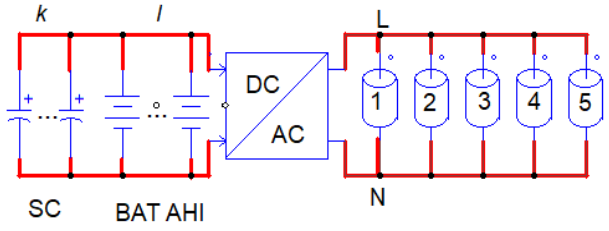

Fig. 16. Scheme of powering household appliances (1- microwave, 2-coffee machine, 3-fridge, 4-lighting, 5 – electric kettle).

In the example it is assumed, that a representative load profile is known as shown in figure 17. The hybrid storage components are: AHI S30-0080 and supercapacitor modules C3000M24, which parameters are presented in table 1 and table 4 respectively.

Table 4. Ultra capacitor C3000M24 parameters

Capacitance	125 F	
Voltage Range	0 to 68,4 V	
Nominal Voltage	64.8 V	
Resistance	Max. 6.7 mΩ	
Stored energy	Initial	72,9 Wh
	End of life	58,3 Wh
Max. Continuous Current	ΔT=15°C	100 A
	ΔT=40°C	180 A
Current	Leakage	<27 mA
Temperature	Operating	-40 ~ +65 °C
	Storage	-40 ~ +70 °C
Cycle Life (25°C)	After 1 000 000 cycles between rated voltage to half rated voltage at +25 °C	
	Capacitance change	<20% decrease
	Internal resistance change	<100% increase
Weight	21 ± 1 kg	

The C3000M24 supercapacitor is voltage-matched to the AHI battery. Alternatively, it may be replaced by four LSUM016R2C0500F modules connected in series. Modules

of this type are available from many different manufacturers (Maxwell, Wima, LS Mtron). The initial parameters for the algorithm (Fig. 15) are shown in table 5.

Table 5. Initial parameters

Maximum instantaneous power of load profile	P_{p_MAX}=2600W
Energy of load profile	E_p=1.723kWh
Stored energy (I_{bat}=10A discharge current)	E_{bat}=1.55 kWh
Discharge capacity (I_{bat}=10A discharge current)	Q_C=37Ah
Minimum battery voltage	U_{bat_min}=40V
Maximum battery current	I_{bat_max}=17A
Maximum continuous battery power	P_{bat_max}=680W
Converter efficiency	η= 95%
Initial number of batteries	l_0=5 (equitation 12)
Cost per single SC module	C_{sc}=1400$
Cost per single BAT module	C_{bat}=950$
Mass of single SC module	M_{sc}=21kg
Mass of single BAT module	M_{bat}=118kg

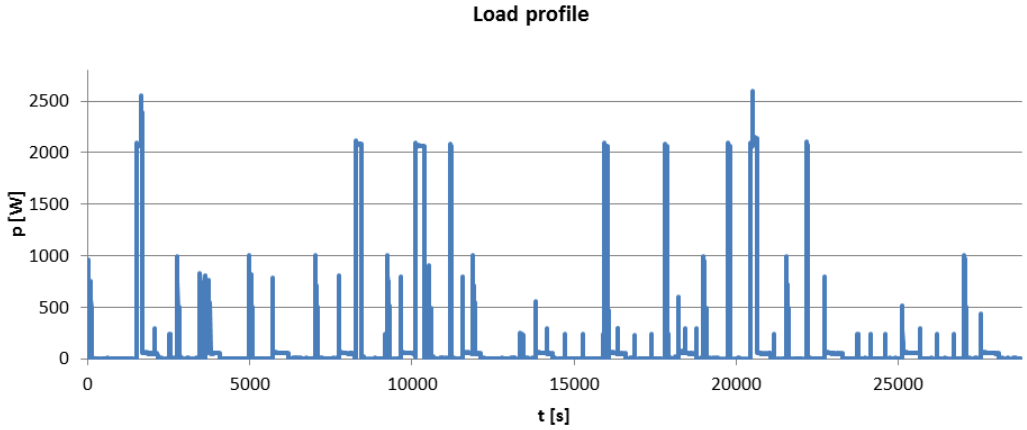

Fig. 17. Profile of the load generated by the work of household appliances

Starting with the initial values l_M = 5 and k = 0 (evaluated by formula (12)), the following results were obtained:

1. According to the cost criterion l_C =5 k_C = 0
$F_{C_{\text{MIN}}} = F_C(k_C, l_C)$ =$ 4750 (mass 590 kg)

2. According to the mass criterion l_M =2 k_M = 3
$F_{M_{\text{MIN}}} = F_M(k_M, l_M)$ =299 kg (cost $ 6100)

As shown in the example given, the knowledge of the load profile has a significant influence on the choice of the storage configuration.

If one considers the need to replace AHI batteries in service, then the configuration of the hybrid storage for the cost will be the same as the configuration obtained by the mass criterion.

Fig. 18. Laboratory setup for storage testing

Conclusion

This article describes how to create an AHI battery model and then use it to design a hybrid storage. The model validation was based on a real storage composed of AHI S30-0080 battery coupled to the 129R6C 0062F EA supercapacitor. A photo of the laboratory setup is shown in figure 18.

Based on the conducted experiment, a simulation error in the voltage and current projection of the hybrid storage was estimated. The maximum errors value for the voltage and current were 2% (mean value 0.27%) and 3.2% (mean value 0.35%) respectively. It has been shown, that in addition to the knowledge of mathematical models of components, the load profile is necessary to properly design the hybrid storage. A statistically representative profile makes it possible to optimize the structure for cost or total weight of the device. The hybrid storage configuration obtained from the proposed calculation method expresses a compromise between the cost and the acceptable probability of continuity of power supply.

The described way of selecting the components of a hybrid storage is mainly used for pulsed loads. The example deals with this type of load. The pulsed loads are caused by either short-time acting devices (e.g. coffee machines) or work coincidence (e.g. switching on the refrigerator and water heater). The example shows that the use of supercapacitors enables the construction of a storage nearly two times lighter than that with AHI battery only (590 kg only AHI, 299 kg SC + AHI). However, due to the cost of implementation, so far, the solution containing only batteries is cheaper.

The presented optimization method can be applied to more complex structures containing different types of batteries. It is expected that the connection of the AHI battery with the supercapacitor also has an effect on extending battery life. This may be due to limiting the value of the current pulses of the AHI battery during charging and discharging. The beneficial effect of such a combination on lead acid batteries has been demonstrated, among others,

in [21] and [3]. Up to now, there is no research on the aging effects of AHI batteries combined with supercapacitors.

Acknowledgements
The authors thank EMU Sp. z.o.o company for providing two AHI S30-0080 batteries for the research.

***Authors**: mgr inż. Monika Liedke, E-mail: monika.liedke@iel.pl; dr inż. Eugeniusz Łowiec, E-mail: eugeniusz.lowiec@iel.pl; mgr inż. Leszek Wolski, E-mail: leszek.wolski@iel.pl; prof. dr hab. inż. Ryszard Strzelecki, E-mail: ryszard.strzelecki@iel.pl; Instytut Elektrotechniki, Bałtycka Pracownia Technologii Energoelektronicznych w Gdyni, ul. Czechosłowacka 3, 81-336 Gdynia, mgr inż. Wojciech Matelski, Politechnika Gdańska, Wydział Elektrotechniki i Automatyki, Katedra Energoelektroniki i Maszyn Elektrycznych, ul. G. Narutowicza 11/12, 80-216 Gdańsk, E-mail: wojciech.matelski@pg.edu.pl*

REFERENCES

[1] Whitacre J. F. et al, A Polyionic, Large-Format Energy Storage Device Using an Aqueous Electrolyte and Thick-Format Composite NaTi2(PO4)3/Activated Carbon Negative Electrodes, *Energy Technology* (2015), 3, 20-31

[2] Sullivan J.L., Gaines L., A Review of Battery Life-Cycle Analysis: State of Knowledge and Critical Needs, *Center for Transportation Research Energy Systems Division, Argonne National Laboratory* , ANL/ESD/10-7 (2010), 8-30

[3] Lahbib I., Lahyani A., Sari A., Venet P., Performance analysis of a lead-acid battery/supercapacitors hybrid and a battery stand-alone under pulsed loads, *2014 First International Conference on Green Energy ICGE,* (2014) 273-278

[4] Lahyani A., Venet P., Guermaz A., Troudi A., Battery/Supercapacitors Combination in Uninterruptible Power Supply (UPS), *IEEE Transactions On Power Electronics*,(2013) VOL. 28, NO. 4, 1509-1522

[5] Mahmudi M., Gazwi A., Battery/Supercapacitor Combinations for Supplying Vehicle Electrical and Electronic Loads, *International Journal of Electronics and Electrical Engineering,* (2014) Vol. 2, No. 2, 153-162

[6] Bentley P., Stone D. A.,The parallel combination of a valve regulated lead acid cell and supercapacitor for use as a hybrid vehicle peak power buffer. *The University Of Sheffield* , *EPE Dresen* (2005),1-10

[7] Pay S., Baghzouz Y.**,** Effectiveness of Battery-Supercapaicitor Combination in Electric Vehicles,*IEEE Bologna PowerTech Conference,* (2003) 1-6

[8] Zhou H., Bhattacharya T.,Tran, D. ,Sing T., Siew T., Composite Energy Storage System Involving Battery and Ultracapacitor With Dynamic Energy Management in Microgrid Applications, *IEEE Transactions On Power Electronics*, VOL. 26, NO. 3, (2011) 923-930

[9] Kim Y., Raghunathan V., Raghunathan A., Design and Management of Battery-Supercapacitor Hybrid Electrical Energy Storage Systems for Regulation Services, *IEEE Transactions On Multi-Scale Computing Systems* ,Vol. 3, No. 1,(2017),12-24

[10] McKeon B., Furukawa J., Fenstermacher S., Advanced Lead–Acid Batteries and the Development of Grid-Scale Energy Storage Systems, *Proceedings of the IEEE* Vol. 102, No. 6, (2014), 951-963

[11] http://wattstor.com/wp-content/uploads/2016/03/Aqueous-Hybrid-Ion-Battery-Data-Sheet.pdf

[12] Li S. , Ke B., Study of Battery Modeling using Mathematical and Circuit Oriented Approaches, *IEEE* (2011), 1-8

[13] Jantharamin N., Zhangt. L., *A* New Dynamic Model *for* Lead-Acid Batteries, *School of Electronic and Electrical Engineering, University of Leeds, U K, IEEE*, (2008), 86-90

[14] Tremblay O., Dessaint L., Experimental Validation of a Battery Dynamic Model for EV Applications, *World Electric Vehicle Journal* Vol. 3 (2009), 289-298

[15] Haddad R., Shahat, A. Kalaani *Y.,* Lead Acid Battery Modeling For Photovoltiac Applications, *Journal of Electrical Engineering* ,6 (2015), 1-8

[16] http://wattstor.com/wp-content/uploads/2016/03/Aqueous-Hybrid-Ion-Battery-Data-Sheet.pdf

[17] https://powersimtech.com/drive/uploads/2016/03/Tutorial-Ultracapacitor-Model-1.pdf

[18] Liu, Z.; Chen, Y.; Luo, Y.; Zhao, G.; Jin, X. Optimized Planning of Power Source Capacity in Microgrid, Considering Combinations of Energy Storage Devices, *Applied. Sciences*. 6, 416 (2016), 1-19

[19] Koohi-Kamali S., Rahima, N. A. Mokhlisa H., New algorithms to size and protect battery energy storage plant in smart microgrid considering intermittency in load and generation, *3rd IET International Conference on Clean Energy and Technology CEAT* (2014), 1-7

[20] Atia R.,Yamada N.,Sizing and Analysis of Renewable Energy and Battery Systems in Residential Microgrids, *IEEE Transactions On Smart Grid*, Vol. 7, No. 3,(2016), 1204-1213

[21] Omar N., Van Mulders F., et al, Effectiveness evaluation of a Supercapacitor-battery parallel combination for Hybrid Heavy Lift Trucks, *EVS24 International Battery, Hybrid and Fuel Cell Electric Vehicle Symposium*, (2009), 1-11

.